An Enhanced Islanding Microgrid Reactive Power, Imbalance Power, and Harmonic Power Sharing Scheme

Jinwei He, Yun Wei Li, *Senior Member, IEEE*, and Frede Blaabjerg, *Fellow, IEEE*

***Abstract*—To address inaccurate power sharing problems in autonomous islanding microgrids, an enhanced droop control method through online virtual impedance adjustment is proposed. First, a term associated with DG reactive power, imbalance power, or harmonic power is added to the conventional real power-frequency droop control. The transient real power variations caused by this term are captured to realize DG series virtual impedance tuning. With the regulation of DG virtual impedance at fundamental positive sequence, fundamental negative sequence, and harmonic frequencies, an accurate power sharing can be realized at the steady state. In order to activate the compensation scheme in multiple DG units in a synchronized manner, a low-bandwidth communication bus is adopted to send the compensation command from a microgrid central controller to DG unit local controllers, without involving any information from DG unit local controllers. The feasibility of the proposed method is verified by simulated and experimental results from a low-power three-phase microgrid prototype.**

***Index Terms*—Distributed generation, droop control, islanding operation, load sharing, microgrid, power sharing, renewable energy system, virtual impedance, voltage control.**

I. Introduction

DISTRIBUTED generation (DG) using renewable energy resource (RES) has been widely used in the recent years. As a DG unit is normally connected to a distribution system with power electronics-based interface, the control of power electronics converter is the key for the robust integration of DG units [1], [2]. When a number of DG units are clustered together, they can also form a microgrid that provides power to critical loads in a distribution network [3]–[7]. In contrast to a conventional distribution system, a microgrid can switch to autonomous islanding operation during main grid faults and a direct voltage support can be provided by DG interfacing converters.

In the case of islanding operation, the load demand must be properly shared by parallel DG units. To facilitate the power sharing requirement without using any communications between DG units, the real power–frequency and reactive power–voltage magnitude droop control method has been developed [3]–[10], [13], and [24]. In this control category, real power and reactive power in the power control loop are calculated using low-pass filters (LPF). Accordingly, the major focus of droop control is the sharing of averaged real and reactive power. It has been pointed out that the real power sharing is always accurate, while the reactive power sharing performance is dependent on the impedance of DG feeders [3]. In addition, the droop control method may cause some stability problems when DG feeders are mainly resistive [16], [28]. To enhance the power sharing performance in a microgrid, various types of modified droop control methods have been developed. In [4], a DG unit is equipped with dominate inductive virtual impedance. With this method, the reactive power sharing errors can be reduced. However, in a weak islanding microgrid with higher existing feeder impedance, the virtual impedance needs to be very large, and therefore, the power sharing dynamics can be affected. To avoid the using of virtual impedance, a few alternatively methods have been developed. In [36], an interesting "Q-V dot droop" method was proposed. However, it can be seen that the reactive power sharing errors can hardly be completely eliminated using the method in [36], especially in the case of a weak microgrid. Additionally, an improved droop control method [19] was proposed to realize the power sharing in proportion to DG power rating. Compared to the standard droop control method, the power sharing performance in [19] is improved via the measurement of point of common coupling (PCC) voltage. Furthermore, virtual, real, and reactive power concept was introduced in [37] to improve the stability of droop control. Similarly, the concept of virtual frequency and virtual voltage magnitude concept [38] was also proposed to prevent instability operation of islanding microgrids.

Note that for a microgrid with intensive nonlinear or imbalanced loads, the circulating imbalance and harmonic current among DG units cannot be directly addressed by the conventional droop control. To alleviate current circulation problem, virtual impedance shaping method was also developed to adjust DG equivalent impedance at fundamental negative sequence [12] and harmonic frequencies [19], [23], [35]. Similar to the situation of reactive power load sharing, mismatched feeder impedance in a weak microgrid also affects imbalance power and harmonic power sharing performance even when the virtual impedance is used.

Manuscript received September 10, 2013; revised May 10, 2014; accepted June 13, 2014. Date of publication June 25, 2014; date of current version January 16, 2015. This paper was presented in part at the 5th IEEE Energy Conversion Congress and Exposition, 2013, Denver, CO, USA. Recommended for publication by Associate Editor J. Liu.

J. He is with Accuenergy Canada Inc., Toronto, ON T6G 2V4 Canada (e-mail: hjinwei@ualberta.ca).

Y. W. Li is with the University of Alberta, Edmonton, AB T6G 2V4 Canada (e-mail: yunwei.li@ ualberta.ca).

F. Blaabjerg is with Aalborg University, 9220 Aalborg, Denmark (e-mail: fbl@et.aau.dk).

Color versions of one or more of the figures in this paper are available online at http://ieeexplore.ieee.org.

Digital Object Identifier 10.1109/TPEL.2014.2332998

Thanks to the emerging low-bandwidth communication-aided microgrid concept [6], [14], [18], [29]–[34], there are also opportunities to further reduce the microgrid load demand sharing errors by actively compensating the impact of feeder impedance. In [30] and [31], a central controller is implemented at a microgrid to detect the PCC voltage or load/grid current. These measured steady-state PCC signals are modulated to dc quantities at their corresponding synchronous rotating frames. At each DG unit local controller, dc signals are switched back to ac signals by a few signal demodulators. An important advantage of this method is that harmonic signals can be transmitted to a DG unit local controller by using a low-bandwidth communication system with around 1000 Hz sampling frequency. In addition, with the help of low-bandwidth communication, hierarchical control architecture is proposed in order to achieve better control, management, and operation of microgrid [33], 34]. To identify the reactive power sharing error without measuring PCC voltage, the real power and reactive power control are coupled by using a modified droop control in [8]. When the reactive power sharing errors are detected, it can be eliminated by using a simple intermittent integral term that adjusts the DG voltage magnitude. However, only reactive power sharing problem is addressed in [8]. For an islanding microgrid with a large number of nonlinear or imbalanced loads, developing a schematic compensation method to realize accurate reactive, imbalance, and harmonic power sharing is very necessary.

In this paper, an adaptive virtual impedance control method is applied to DG units in islanding microgrids. The virtual impedance at fundamental positive sequence, fundamental negative sequence, and harmonic frequencies are determined according to transient real power variations. To activate small amount of transient power variations, a transient control term is added to the conventional real power–frequency droop control. Through interactions between real power variations and the virtual impedance regulation, a microgrid reactive power, imbalance power, and harmonic power sharing errors can be compensated at the steady state.

II. Microgrid System Structure

A. Principle of Microgrid Power Sharing

Fig. 1 shows a simplified diagram of an islanding microgrid, where a few DG units are integrated into the microgrid with *LC* filters. For each DG unit, the backstage power is provided by a RES or an energy storage system. To simplify the discussion, an infinite dc link with fixed dc voltage is assumed in this paper. There are a few linear, imbalanced, and harmonic loads placed at the PCC. A microgrid central controller is also placed at PCC. To realize the proposed compensation scheme in DG units in a synchronized manner, a central controller is adopted to send synchronized compensation flag signals to DG local controllers.

At a DG unit local controller, the traditional real power–frequency droop control and reactive power–voltage magnitude droop control are adopted as

$$f_{\mathrm{DG}} = f^* - D_P \cdot P_{\mathrm{LPF}} \tag{1}$$

$$E_{\mathrm{DG}} = E^* - D_q \cdot Q_{\mathrm{LPF}} \tag{2}$$

where f^* and f_{DG} are the DG nominal and reference frequencies. E^* and E_{DG} are the DG nominal and reference voltage magnitudes. D_p and D_q are the droop coefficients for controlling DG real power P_{LPF} and reactive power Q_{LPF}, respectively. With the frequency and the voltage magnitude reference, instantaneous DG voltage references $V_{\mathrm{droop}\_\alpha}$ and V_{droop_β} in the two-axis stationary reference frame can be obtained by using a reference generator.

As mentioned earlier, the stability and dynamic performance of the conventional droop control is a subject to the impact of DG feeders. To alleviate the impact of feeder impedance, the static virtual impedance [3], [16] was proposed by deducting a voltage drop term from the voltage reference as

$$V_{\mathrm{ref}\_\alpha} = V_{\mathrm{droop}\_\alpha} - (\omega_0 L_V I_\beta + R_V I_\alpha) \tag{3}$$

$$V_{\mathrm{ref}\_\beta} = V_{\mathrm{droop}\_\beta} - (-\omega_0 L_V I_\alpha + R_V I_\beta) \tag{4}$$

where V_{ref_α} and V_{ref_β} are the voltage references considering the control of virtual impedance. L_V and R_V are the static virtual inductance and resistance, respectively. I_α and I_β are the DG unit current in the stationary two-axis reference frame. Note that the virtual impedance control in (3) and (4) mainly focuses on the performance of the DG unit at the fundamental frequency.

Afterward, a high-bandwidth voltage controller [21], [22] is needed for tracking the voltage references in (3) and (4).

B. Analysis of Reactive, Imbalance, and Harmonic Power Sharing Errors

The previous section reviewed how the conventional droop control and the static virtual impedance regulation are applied to a DG unit. In this section, the sharing of a microgrid load demand is discussed by investigating on a simplified DG equivalent circuit.

Fig. 2 illustrates an equivalent circuit of an islanding microgrid with two droop controlled DG units. It can be seen from Fig. 2(a) that DG units are modeled by controlled voltage sources and series virtual impedances at fundamental positive sequence. Meanwhile, the PCC load is lumped as a passive *RL* load. In order to realize accurate real and reactive power sharing, DG units at the same power rating shall design the droop control slopes according to [13]. In addition, the same fundamental positive sequence equivalent impedance shall be controlled in both DG units. In the case of Fig. 2(a), the fundamental positive sequence equivalent impedance is defined as the series combination of existing physical feeder impedance and the virtual impedance controlled by the DG unit

$$L_f = L_{\mathrm{phy},f} + L_{v,f} \tag{5}$$

$$R_f = R_{\mathrm{phy},y} + R_{v,f} \tag{6}$$

where L_f and R_f are the DG equivalent inductance and resistance at the fundamental positive sequence. $L_{\mathrm{phy},f}$ and $R_{\mathrm{phy},f}$ are the physical feeder inductance and resistance at the fundamental positive sequence. $L_{V,f}$ and $R_{V,f}$ are the fundamental positive sequence virtual impedance controlled by the DG unit.

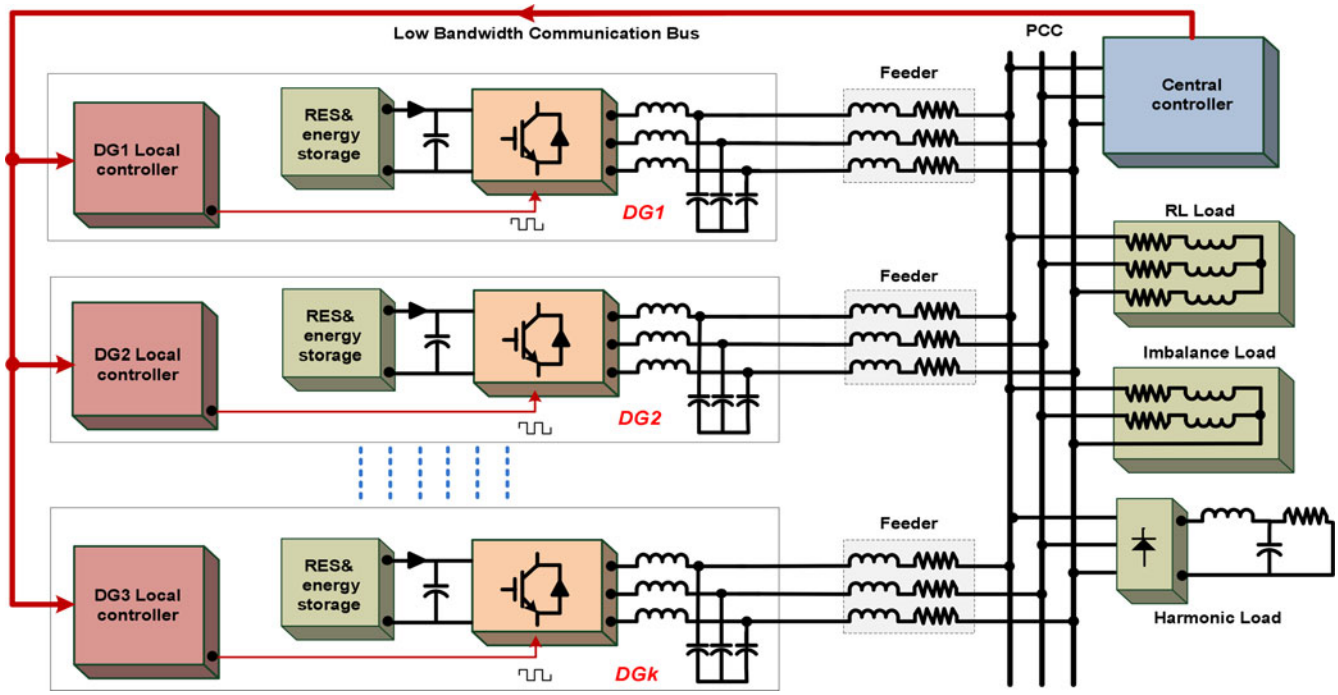

Fig. 1. Diagram of an islanding microgrid with one-way low-bandwidth communication.

In addition, the equivalent circuit at fundamental negative sequence is presented in Fig. 2 (b), where the PCC imbalanced load is described as a current source (I_{Neg}) [12]. In this system, the equivalent fundamental negative sequence DG impedance is

$$L_{\mathrm{Neg}} = L_{\mathrm{phy,Neg}} + L_{v,\mathrm{Neg}} \tag{7}$$

$$R_{\mathrm{Neg}} = R_{\mathrm{phy,Neg}} + R_{v,\mathrm{Neg}} \tag{8}$$

where $L_{\mathrm{phy,Neg}}$ and $R_{\mathrm{phy,Neg}}$ are the inductance and resistance of physical feeder at fundamental negative sequence. To share the imbalance load current using multiple DG units, the equivalent fundamental negative sequence impedance L_{Neg} and R_{Neg} are regulated by controlling DG virtual impedance $L_{V,\mathrm{Neg}}$ and $R_{V,\mathrm{Neg}}$ at the fundamental negative sequence.

Finally, the equivalent circuit at harmonic frequencies is given in Fig. 2(c) as

$$L_H = L_{\mathrm{phy},H} + L_{V,H} \tag{9}$$

$$R_H = R_{\mathrm{phy},H} + R_{V,H} \tag{10}$$

where L_H and R_H are the DG equivalent inductance and resistance at harmonic frequencies. The physical feeder impedance is described as $L_{\mathrm{phy},H}$ and $R_{\mathrm{phy},H}$. $L_{V,H}$ and $R_{V,H}$ are the harmonic virtual impedance controlled by DG units.

To simplify the discussion, this paper assumes that DG units in an islanding microgrid are interfaced to PCC with inductive physical feeders. This is because series coupling chokes are normally required in the droop controlled DG units, in order to ensure the stability of power sharing control. In addition, DG units are often interconnected to a distribution system with isolation transformers, which have highly inductive leakage impedance. Finally, even for some directly coupled DG units with only *LC* filters, the fixed value inductive virtual impedance can be preactivated through DG unit virtual impedance control scheme. As it will be discussed later, DG unit virtual impedance in this case is the series combination of preactivated virtual impedance and the adaptive virtual impedance that is adjusted by the proposed compensation scheme. If the ranges of adaptive virtual impedance and preactivated virtual inductance are both properly designed, the DG equivalent impedance can be always inductive at fundamental and selected harmonic frequencies.

Based on the assumption of inductive DG equivalent impedance and slow microgrid load demand dynamics [8], 24], the relationship between DG output power and DG equivalent inductance can be summarized as

$$\begin{cases} L_f \uparrow & Q_{\mathrm{LPF}} \downarrow \\ L_{\mathrm{Neg}} \uparrow & Q_{\mathrm{Neg}} \downarrow \\ L_H \uparrow & Q_{\mathrm{Har}} \downarrow \end{cases} \tag{11}$$

where Q_{LPF}, Q_{Neg}, and Q_{Har} are DG unit reactive power, imbalance power, and harmonic power, respectively. Their detailed definition is given in next section. Based on (11) and the aforementioned discussion, it can be seen that the output power of a DG unit decreases when the corresponding equivalent DG inductance increases and *vice versa*.

III. Proposed Power Sharing Enhancement Method

As discussed in the previous section, the control of DG equivalent inductance can adjust the power sharing performance of the microgrid. However, determining the desired DG equivalent impedance requires the knowledge of equivalent impedance of other DG units. In addition, the DG unit existing feeder impedance also needs to be known by the DG unit local controller. But the detection of DG physical feeder impedance can

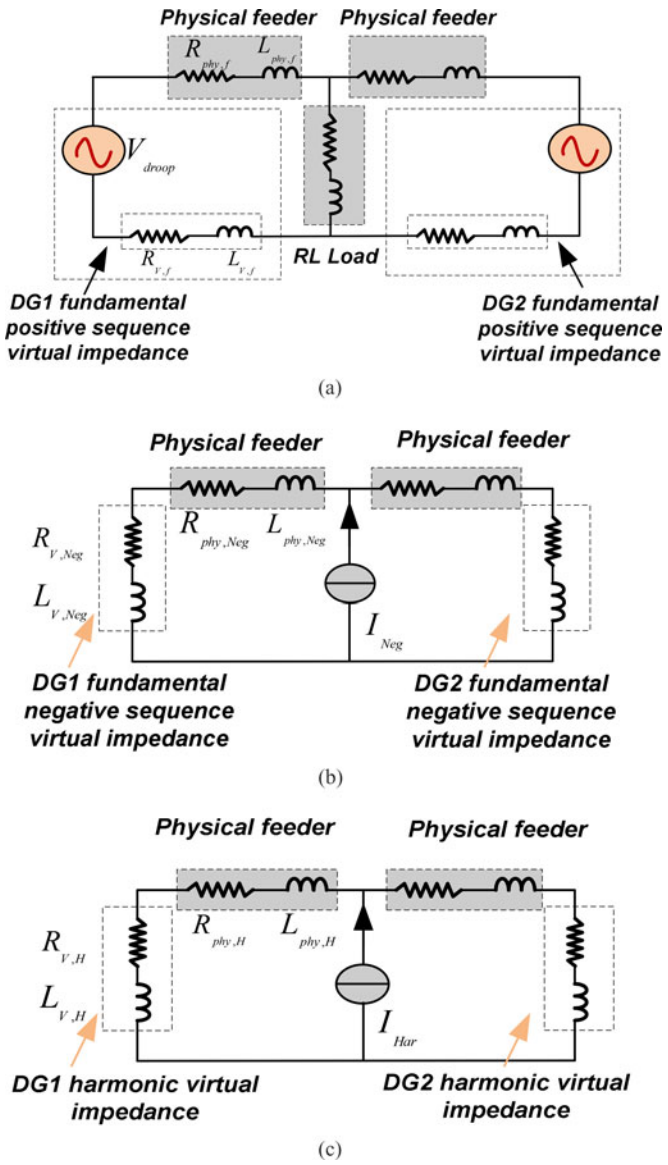

Fig. 2. Equivalent circuits of a microgrid at different frequencies and sequences. (a) Equivalent circuit at fundamental positive sequence. (b) Equivalent circuit at fundamental negative sequence. (c) Equivalent circuit at harmonic frequencies.

increase the computational load of DG local controllers. In this section, the microgrid frequency is utilized as a link between parallel DG units, and the transient real power variations are used to adjust the DG unit equivalent impedance. With the proposed method, the detection of DG existing feeder impedance is unnecessary for the power sharing error compensation.

A. DG Unit Power Calculation

First, the fundamental positive sequence, fundamental negative sequence, and harmonic components of DG current are separated by using the second-order generalized integrator [11] and the delayed-signal cancellation [15] based sequence decomposition method. A simplified detection diagram is sketched in Fig. 3. With the detected current components, the output power

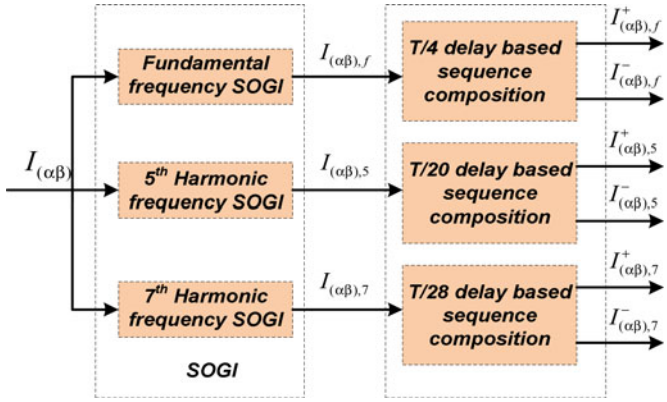

Fig. 3. Decomposition of fundamental positive sequence, fundamental negative sequence, and harmonic components. T is the fundamental cycle.

of a three-phase DG unit can be calculated as

$$P_{\mathrm{LPF}} = \frac{3}{2(\tau s+1)} \cdot (V_{\mathrm{DG},\alpha} \cdot I^{+}_{\alpha,f} + V_{\mathrm{DG},\beta} \cdot I^{+}_{\beta,f}) \tag{12}$$

$$Q_{\mathrm{LPF}} = \frac{3}{2(\tau s+1)} \cdot (V_{\mathrm{DG},\beta} \cdot I^{+}_{\alpha,f} - V_{\mathrm{DG},\alpha} \cdot I^{+}_{\beta,f}) \tag{13}$$

$$Q_{\mathrm{Har}} = 3/2 \cdot E^{*} \cdot \sqrt{(I^{-}_{\alpha,5})^2 + (I^{-}_{\beta,5})^2 + (I^{+}_{\alpha,7})^2 + (I^{+}_{\beta,7})^2} \tag{14}$$

$$Q_{\mathrm{Neg}} = 3/2 \cdot E^{*} \cdot \sqrt{(I^{-}_{\alpha,f})^2 + (I^{-}_{\beta,f})^2} \tag{15}$$

where P_{LPF} is the DG real power and Q_{LPF} is the DG reactive power. The ripples in DG real and reactive power are attenuated by using LPFs with time constant τ [17]. Q_{Har} and Q_{Neg} are defined as DG harmonic power and imbalance power, respectively. E^{*} is the rated DG phase voltage (peak value). $V_{\mathrm{DG},\alpha}$ and $V_{\mathrm{DG},\beta}$ are the measured DG voltages in the stationary reference frame. $I^{+}_{\alpha,f}$ and $I^{+}_{\beta,f}$ are the DG fundamental positive sequence current, $I^{-}_{\alpha,f}$ and $I^{-}_{\beta,f}$ are the DG fundamental negative sequence current. $I^{-}_{\alpha,5}$ and $I^{-}_{\beta,5}$ are the negative sequence component of DG fifth harmonic current. $I^{+}_{\alpha,7}$ and $I^{+}_{\beta,7}$ are the positive sequence component of DG seventh harmonic current. Note that in this paper, only dominate low order harmonic currents are adopted to calculate the harmonic power.

B. Couplings Between DG Unit Virtual Impedance and Transient Droop Control

It has been demonstrated that the conventional frequency droop control in (1) can realize zero steady-state real power sharing errors [3]. Therefore, when a disturbance term associated with reactive power Q_{LPF}, harmonic power Q_{Har}, or imbalance power Q_{Neg} is added to the frequency droop control in (1), the real power sharing shall appear some variations when Q_{LPF}, Q_{Har}, or Q_{Neg} in multiple DG units are not the same. For the same reason, if these load demands are properly shared by DG units, adding the same amount of frequency disturbance to (1) will not cause any obvious real power variations. Therefore, one can find that the transient real power variations indirectly

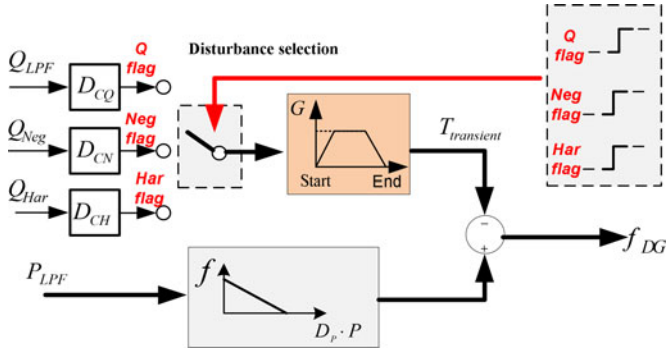

Fig. 4. Real power disturbance injection during the compensation (step 2).

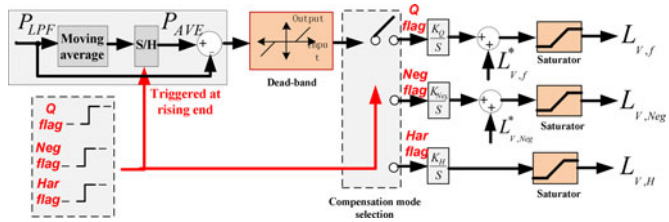

Fig. 5. DG virtual impedance adjustment during the compensation (step 3).

indicate the reactive, harmonic, and imbalance power sharing errors in an islanding microgrid.

Based on the above discussions and the analysis of DG equivalent circuit in Fig. 2, it is practical to eliminate the power sharing errors by injecting couplings between the transient real power variations and the DG virtual impedance.

The proposed power sharing error compensation scheme is composed of the following three steps.

Step 1 (Conventional droop control): First, the conventional droop control scheme as shown in (1) and (2) is applied to the microgrid. In this step, the DG unit monitors the compensation signals coming from the central controller. Once the DG unit receives a compensation signal, its control mode switches to steps 2 and 3. Note that in the first step, the ripple-free real power $P_{\rm ave}$ is also measured by using an additional moving average filter. And this value is recorded as a reference during the compensation in steps 2 and 3.

Step 2 (Real power disturbance injection): When a compensation flag from the microgrid central controller is received by the DG unit local controller, the DG unit starts power sharing compensation by activating steps 2 and 3 at the same time. Note that the sending of one way compensation flag does not need any information of DG unit local controllers. Therefore, the communication from DG units to the microgrid central controller is not necessary. In step 2, a transient disturbance term associated with reactive power, imbalance power, or harmonic power is slowly deducted from the frequency control. Accordingly, the conventional droop control is modified as

$$f_{\rm DG} = f^* - D_P \cdot P_{\rm LPF} - T_{\rm transient} \tag{16}$$

$$E_{\rm DG} = E^* - D_q \cdot Q_{\rm LPF} \tag{17}$$

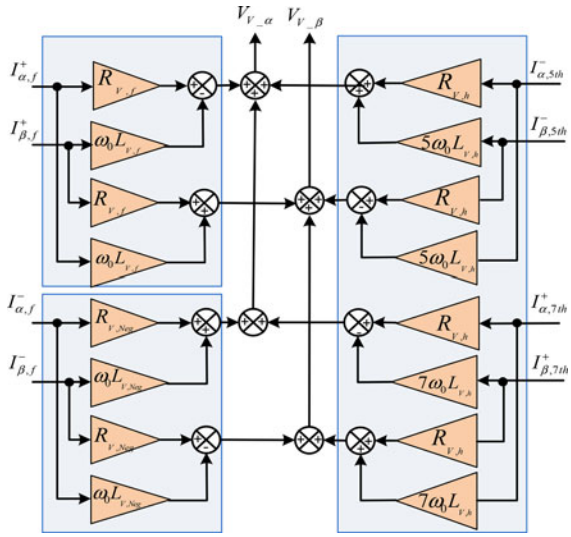

Fig. 6. Implementation of virtual impedance at fundamental positive sequence, fundamental negative sequence, and harmonic frequencies.

where the transient disturbance term $T_{\rm transient}$ is determined by the type of compensation flag signal from the microgrid central controller. It has three options depending on how the flag signal from central controller is

$$T_{\rm transient} = \begin{cases} G \cdot (D_{\rm CQ} \cdot Q_{\rm LPF}) & \text{Reactive power flag (Q flag)} \\ G \cdot (D_{\rm CN} \cdot Q_{\rm Neg}) & \text{Imbalance power flag (Neg flag)} \\ G \cdot (D_{\rm CH} \cdot Q_{\rm Har}) & \text{Harmonic power flag (Har flag)} \end{cases} \tag{18}$$

where G is a time-varying soft compensation factor [8]. It increases slowly from 0 to 1 at the beginning of the compensation and it reduces to zero at the end of the compensation. The coefficients $D_{\rm CQ}$, $D_{\rm CH}$, and $D_{\rm CN}$ are designed to ensure that appropriate amount of disturbances is injected to the frequency control. It is important to note that the reactive, harmonic, and imbalance power sharing errors cannot be simultaneously compensated by the proposed method. In each compensation transient (steps 2 and 3), only one type of compensation flag can be generated by the microgrid central controller. Fig. 4 presents a detailed diagram of injecting real power disturbance.

Step 3 (Virtual impedance adjustment): When the real power variation is introduced by injecting frequency disturbances, it should be captured to adjust the DG series virtual impedance. This process is defined as step 3. The detailed virtual impedance regulation diagram is shown in Fig. 5.

First, the measured ripple-free DG real power $P_{\rm ave}$ before receiving the compensation flag is saved to identify the real power variations.

As shown in Fig. 5, if the reactive power compensation flag is received by the DG unit, the difference between the measured real power $P_{\rm LPF}$ and the DG real power $P_{\rm ave}$ saved in the end of step 1 is employed to adjust the DG virtual impedance at the

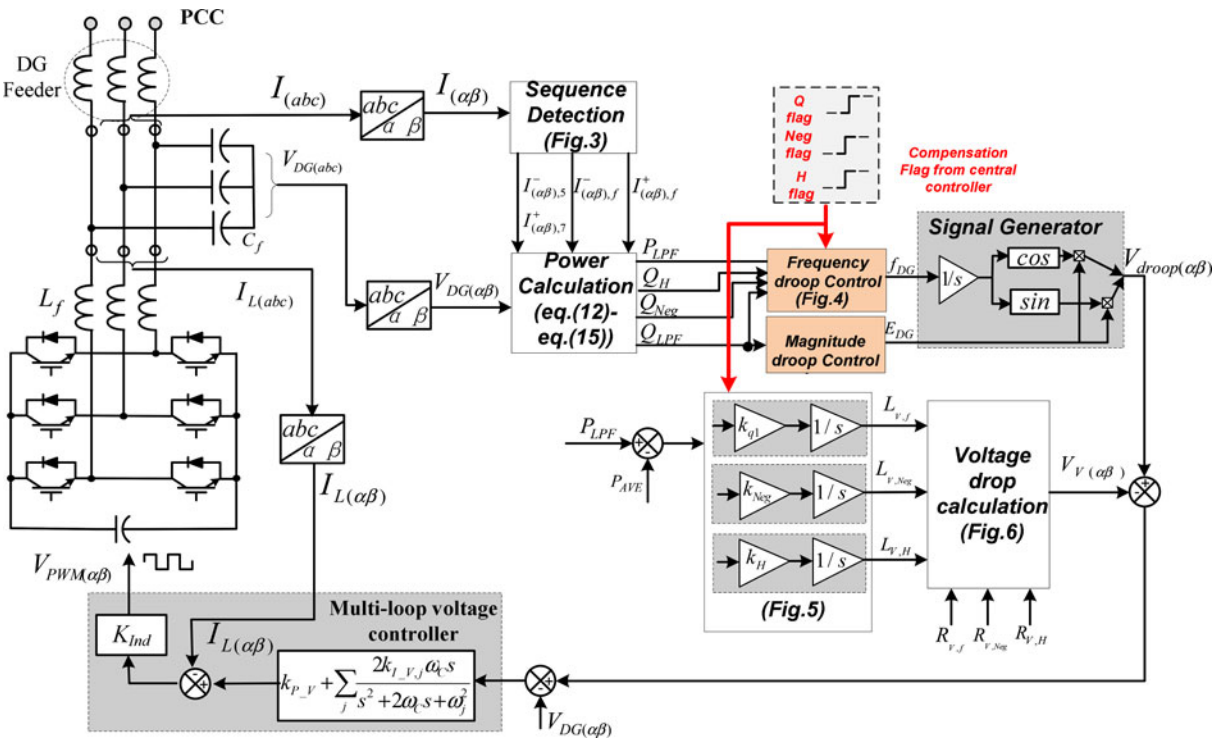

Fig. 7. Complete diagram of a DG unit using the proposed control method.

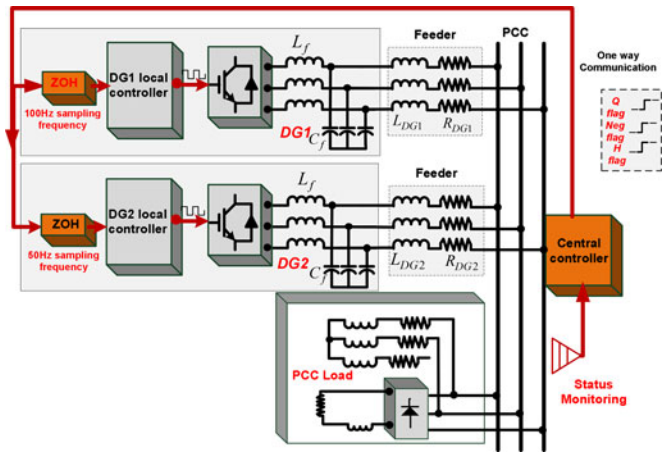

Fig. 8. Diagram of the simulated microgrid with two inverters at the same power rating.

fundamental positive sequence as

$$L_{V,f} = L^{*}_{V,f} - \frac{k_q}{s} \cdot (P_{\mathrm{LPF}} - P_{\mathrm{ave}}) \tag{19}$$

where $L^{*}_{V,f}$ is the static virtual inductance at the fundamental positive sequence. As discussed earlier, this static virtual inductance is used to ensure that the DG equivalent impedance is always inductive at the fundamental positive sequence. $L_{V,f}$ is adjusted by an integral control with the transient real power variations $(P_{\mathrm{LPF}} - P_{\mathrm{ave}})$ as the input.

To get a better understanding of the principle of the proposed compensation scheme, it is assumed that DG1 shares less reactive power in step 1. When the reactive power compensation flag is received by DG1, the real power has some overshoot due to the control scheme in (16). As it has been pointed out that smaller equivalent fundamental positive sequence inductance increases the sharing of reactive power load in this DG unit, the real power overshoot $(P_{\mathrm{LPF}} - P_{\mathrm{ave}})$ are employed as an input to tune the magnitude of virtual inductance at fundamental positive sequence. When the microgrid reactive power load demand is equally shared by multiple DG units, the frequency control in (16) will automatically make the transient real power variation $(P_{\mathrm{LPF}} - P_{\mathrm{ave}})$ reduces to zero, as the same amount of frequency bias is injected by $T_{\mathrm{Transient}}$.

For the same reason, if an imbalance power compensation flag is received by the DG unit local controller, a disturbance $G \cdot D_{\mathrm{CN}} \cdot Q_{\mathrm{Neg}}$ shall be injected to the frequency droop control in (16) and the virtual inductance $L_{V,\mathrm{Neg}}$ at the fundamental negative sequence shall be adjusted in a similar manner as

$$L_{V,\mathrm{Neg}} = L^{*}_{V,\mathrm{Neg}} - \frac{k_{\mathrm{Neg}}}{s} \cdot (P_{\mathrm{LPF}} - P_{\mathrm{ave}}) \tag{20}$$

where $L^{*}_{V,\mathrm{Neg}}$ is a static virtual inductance at the fundamental negative sequence frequency. k_{Neg} is an integral gain to adjust the virtual inductance.

Finally, when the DG unit receives a flag signal to compensate the system harmonic power sharing errors, the real power variation due to the injection of $G \cdot D_{\mathrm{CH}} \cdot Q_{\mathrm{Har}}$ in (16) needs to be captured to regulate the virtual impedance at selected harmonic frequencies as

$$L_{V,H} = -\frac{k_{\mathrm{Har}}}{s} \cdot (P_{\mathrm{LPF}} - P_{\mathrm{ave}}) \tag{21}$$

TABLE I
PARAMETERS IN SIMULATION AND EXPERIMENT

System Parameter	Value
LC filter	$L_f = 3\,\mathrm{mH}$ and $C_f = 25$ uF
DC link voltage	650 V (Simulation), 350 V (Experiment)
Switching frequency	10 kHz
Main grid	380 V (line to line *RMS*) /50 Hz (Simulation), 115 V (line to line *RMS*) /50 Hz (Experiment)
DG feeder	*DG1 Feeder inductance* $L_{\mathrm{DG1}} = 1.5\,\mathrm{mH}$ *DG1 Feeder resistance* $R_{\mathrm{DG1}} = 0.2\,\Omega$, *DG2 Feeder inductance* $L_{\mathrm{DG2}} = 3.5\,\mathrm{mH}$ *DG2 Feeder resistance* $R_{\mathrm{DG2}} = 0.2\,\Omega$
Double-loop voltage control parameter	**Value**
k_{pV}	0.10
k_{ih}	20 ($h = 1$), 15 ($h = 5, 7, 9$), 10 ($h = 11$)
k_{pI}	20
ω_{b}	8
Power control parameter	**Value**
Real power control D_{p}	Simulation: 5.6×10^{-5} Experiment: 5.0×10^{-4}
Reactive power control D_{q}	Simulation:1.2×10^{-4} Experiment: 1.0×10^{-3}
D_{CQ}	Simulation: 4×10^{-5} Experiment: 6.7×10^{-4}
D_{CH}	Simulation:4×10^{-5} Experiment: 5.0×10^{-4}
D_{CN}	Simulation: 4×10^{-5} Experiment: 1.7×10^{-4}
Real power dead-band in Fig. 5	Simulation: 20 W Experiment: 10 W
k_q	Simulation: 4×10^{-6} Experiment: 1.7×10^{-5}
k_{Har}	Simulation: 4×10^{-6} Experiment: 1.7×10^{-5}
k_{Neg}	Simulation: 4×10^{-6} Experiment: 1.0×10^{-5}
$R_{v,f}$, $R_{v,\mathrm{Neg}}$, and $R_{v,H}$	Simulation: 0.15 Ω Experiment: 0.15 Ω
Load Parameters	**Value**
Load in the simulation	•Three-phase diode rectifier with series inductor and resistor in dc side. •Three-phase Y-connected load bank with phase-c disconnected.
Experiment load type I	•Three-phase Y-connected load bank with phase-c disconnected.
Experiment load type II	•Three-phase diode rectifier with shunt capacitor and resistor in the dc side.
Experiment load typeIII	•Three-phase diode rectifier with shunt capacitor and resistor in the dc side.•Three-phase Y-connected load bank with phase-c disconnected

where $L_{V,H}$ is the virtual inductance at the harmonic frequencies.

Note that the proposed method is developed based on an assumption that real power load in an islanding distribution system is fixed during the compensation process. When there are some real power load demand fluctuations during steps 2 and 3, the proposed method may not be able to completely eliminate reactive power, harmonic power, and imbalanced power sharing errors. To address this concern, the proposed compensation should be activated in very few minutes. With this arrangement, the errors caused by real power fluctuations can be mitigated by other compensations. Additionally, the compensation period shall be properly designed to reduce the possibility of real power variations during the compensation. This can be achieved by tuning the integral gain in the virtual inductance adjustment loop. In this paper, the period of steps 2 and 3 is selected to

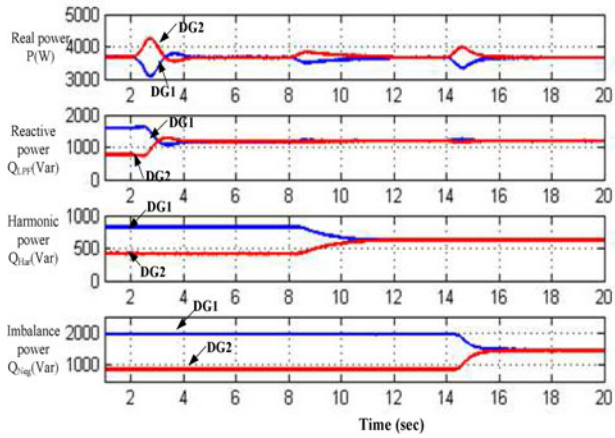

Fig. 9. DG units power flow during the compensation. (From 2.0 to 6.0 s: Reactive power compensation. From 8.0 to 12.0 s: Harmonic power compensation. From 14.0 to 18.0 s: Imbalance power compensation)

be only a few seconds. Considering that the variations of load demand in low voltage residential and commercial distribution systems are normally very slow [25], [26], the proposed method is especially suitable for compensating power sharing errors in islanding commercial or residential microgrids. Finally, it is important to note that only one type of power sharing errors can be mitigated in a compensation transient. There are no priorities between these three compensation flags if they are all implemented in the microgrid. However, if only one type of compensation can be implemented in the microgrid due to the limitations on the communication system or the computational capability of DG unit local controllers, the compensation flag shall be chosen according to PCC load type, DG unit voltage controller performance, and the requirement from islanding microgrid operators.

C. Implementation of Virtual Impedance

Once the virtual impedance is determined by the proposed compensation method, its corresponding voltage drops in the stationary reference frame can be calculated. In the implementation method in [3] and [16], the voltage drop on the fundamental positive sequence virtual impedance is calculated by using control terms with cross-couplings between two-axis stationary reference frame. This idea can be easily extended to implement variable virtual impedances at fundamental negative sequence and harmonic sequences in a similar manner.

A block diagram of the voltage drop calculation is shown in Fig. 6, where $R_{v,f}$, $R_{v,\mathrm{Neg}}$, and $R_{v,H}$ are small virtual resistances at fundamental positive sequence, fundamental negative sequence, and harmonic frequencies, respectively. They are adopted to provide some damping effects to a microgrid [20]. However, further discussion on microgrid damping is out of the scope of this paper.

Similar to the characteristic of the virtual impedance in [3] and [16], the proposed variable virtual impedances as shown in Fig. 6 are implemented without using any differential operations.

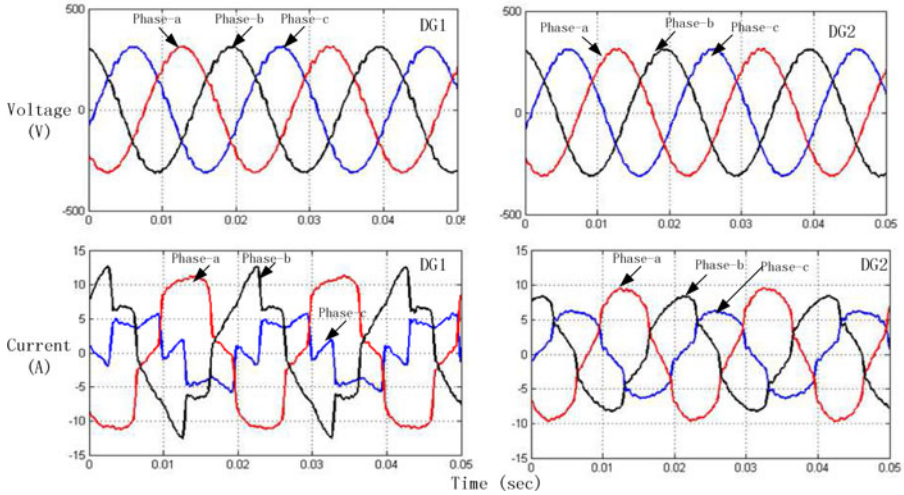

Fig. 10. DG unit phase voltage and phase current with conventional droop control method.

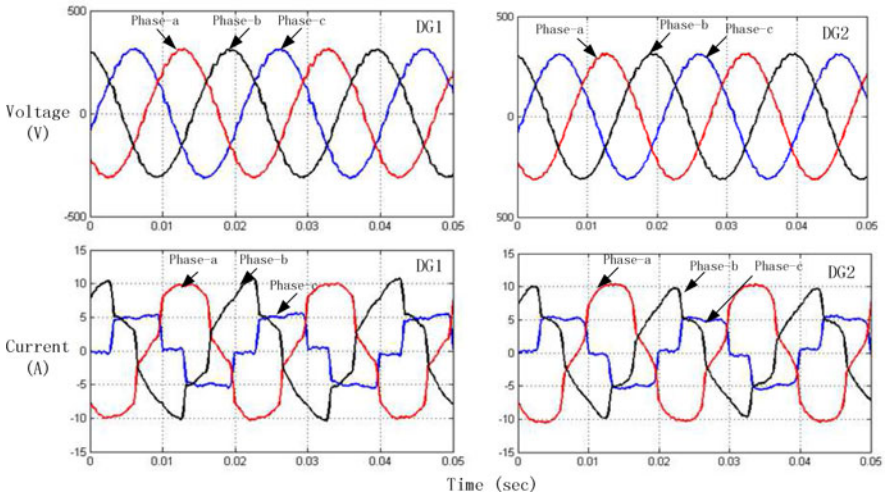

Fig. 11. DG unit phase voltage and phase current after the power sharing errors are compensated by the proposed method.

Therefore, it will not bring additional noises to the DG unit local control system.

D. Closed-Loop DG Voltage Control

To ensure excellent voltage tracking, a double-loop voltage control with harmonic voltage compensators [21], [22] is adopted in this paper. The outer loop is an *LC* filter capacitor voltage control loop ($G_V(s)$) and the inner loop is an inverter output current control loop ($G_I(s)$) as

$$G_V(s) = k_{pV} + \sum_{h=1,5,7.....} \frac{2k_{ih}\omega_b s}{s^2 + 2\omega_b s + (h2\pi f^*)^2} \quad (22)$$

$$G_I(s) = k_{pI} \quad (23)$$

where k_{ih} is the gain of resonant controllers in the outer voltage control loop. ω_b is the bandwidth of the resonant controllers, and k_{pV} is the gain of proportional control. In the inner current control loop, a simple proportional control with gain k_{pI} is adopted. It is important to note that an islanding microgrid power sharing is regulated by controlling the capacitor voltage of DG output *LC* filters. As a result, the primary aim of using a proportional controller in the inner current control loop is to provide sufficient damping to output *LC* filter rather than rapid inverter output current tracking [21], [27].

The complete control diagram of a DG unit is shown in Fig. 7, where the DG local controller receives the compensation commands from the central controller to inject couplings between DG real power and DG virtual impedance. As the proposed virtual impedance adjustment normally takes a few seconds, a few mini-second delay in the communication signals will not affect the accuracy of the proposed compensation method.

IV. Simulation Results

To test the effectiveness of the proposed power sharing method, simulations have been conducted in the MATLAB/Simulink. Two parallel DG units as shown in Fig. 8

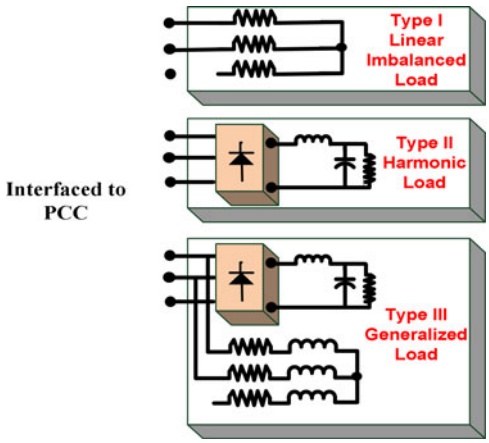

Fig. 12. Three PCC load types in the experimental microgrid. (Type I: Imbalanced load; Type II: Harmonic load; Type III: Generalized load.)

are used in the simulation. The PCC loads are a diode rectifier and a balanced three-phase *RL* load with phase-c disconnected from PCC. The detailed system parameters are provided in Table I.

A. Power Sharing Investigation

First, the power flow of the system is investigated in Fig. 9. From the time range 0 to 2 s, only the conventional droop control using (1) and (2) is adopted. It is obvious that the real power sharing is accurate, but the sharing of reactive power load, imbalance power load, and harmonic power load has some errors.

The performance of the power sharing error compensation can also be seen from Fig. 9. First, the reactive power compensation flag is generated at 2.0 s, followed by the harmonic power compensation flag at 8.0 s and the imbalance power compensation flag at 14.0 s. To demonstrate the effectiveness of the proposed compensation method, compensation flag signals are transmitted to each DG unit local controller via a zero-order hold. The sampling frequencies of zero-order hold are set to 100 Hz for DG unit 1 and 50 Hz for DG unit 2. From 2.0 to 6.0 s, it can be seen that the reactive power sharing errors are effectively compensated. Afterward, the harmonic power sharing errors are mitigated by controlling the DG virtual harmonic impedance. Finally, the imbalance power sharing errors are also compensated through the adjustment of corresponding DG virtual impedance during the time range 14.0 to 18.0 s. Note that during the compensation transient, real power in DG units has some variations due to the injection of frequency disturbance by using (16).

B. DG Voltage and Current Investigation

The corresponding DG phase voltage and phase current are also obtained as shown in Figs. 10 and 11. Fig. 10 presents the performance of DG units before the compensation. It clearly shows that the current waveforms of DG1 and DG2 are not the same. There are some circulating currents between two parallel DG units. This phenomenon is consistent with the DG unit power flow analysis in Fig. 9, where the conventional droop control brings some reactive, harmonic, and imbalance power sharing errors.

When the power sharing errors are compensated using the proposed method, the DG unit voltage and current waveforms are given Fig. 11. Compared to the situation in Fig. 10, Fig. 11 demonstrates that the current sharing errors are effectively eliminated and DG unit 1 and DG unit 2 have similar current waveforms. Note that the proposed method compensates the power sharing errors based on a fact that the total load demand is basically fixed during the compensation process. However, due to the adjustment of virtual impedance in a weak islanding microgrid, it can be seen that the total reactive power demand has a little bit variations during the compensation of imbalance power sharing error and harmonic power sharing error.

V. Experimental Results

Comprehensive experimental results have been obtained from a voltage scaled three-phase microgrid prototype with two parallel DG units at the same power rating. To observe the details of the proposed compensation method, loads as shown in Fig. 12 are connected to PCC. The key parameters of the system are listed in Table I.

Case I (With imbalanced load): First, only a three-phase R load with phase-c floating is connected to PCC. The sharing of load current using conventional droop control method is shown in Fig. 13.

In the case of conventional droop control, the virtual impedance at harmonic frequencies and fundamental negative sequences is not activated and only 1-mH fixed virtual inductance is preactivated at the fundamental positive sequence. Fig. 13 shows that the imbalanced load is not equally shared, and the DG1 phase-a and phase-b current magnitudes are obviously higher than those of DG2. As the PCC load phase-c is disconnected, the DG unit phase-c currents are supposed to be zero under the ideal power sharing condition. However, it can be seen that nontrivial circulating component appears between the phase-c current of DG1 and DG2.

To demonstrate the effectiveness of the proposed method in reducing imbalance power sharing errors, an imbalance power compensation command is produced at the microgrid central controller. After the compensation, an enhanced power sharing performance is shown in Fig. 14, where it can be seen that DG1 current and DG2 current are almost the same.

Case II (With harmonic loads): The sharing of harmonic loads is also examined by an experiment. In this case, the PCC load is a three-phase diode rectifier as shown in Fig. 12. Fig. 15 shows the performance of the microgrid when the control of the harmonic virtual impedance is not activated. As illustrated, DG unit 1 provides more harmonic current as it has smaller existing feeder inductance. When the adjustment of harmonic virtual impedance using (16) and (21) is performed, the improved sharing performance can be seen in Fig. 16. Note that in this case, only the virtual harmonic impedance at the fifth and seventh harmonic frequencies are controlled, as dominate harmonic

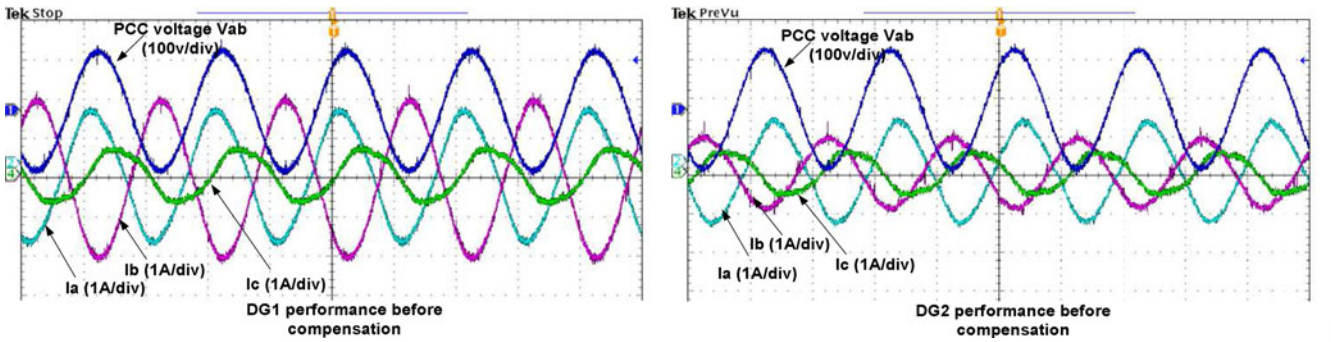

Fig. 13. Performance of the conventional droop control in a microgrid with imbalanced resistive load (load Type I in Fig. 12).

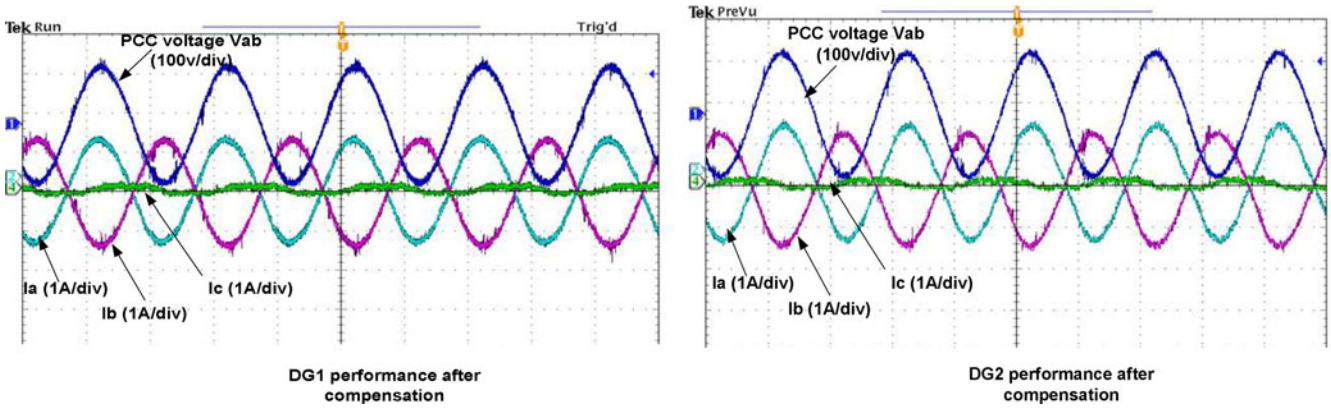

Fig. 14. Performance of the proposed compensation method in a microgrid with imbalanced resistive load (load Type I in Fig. 12)

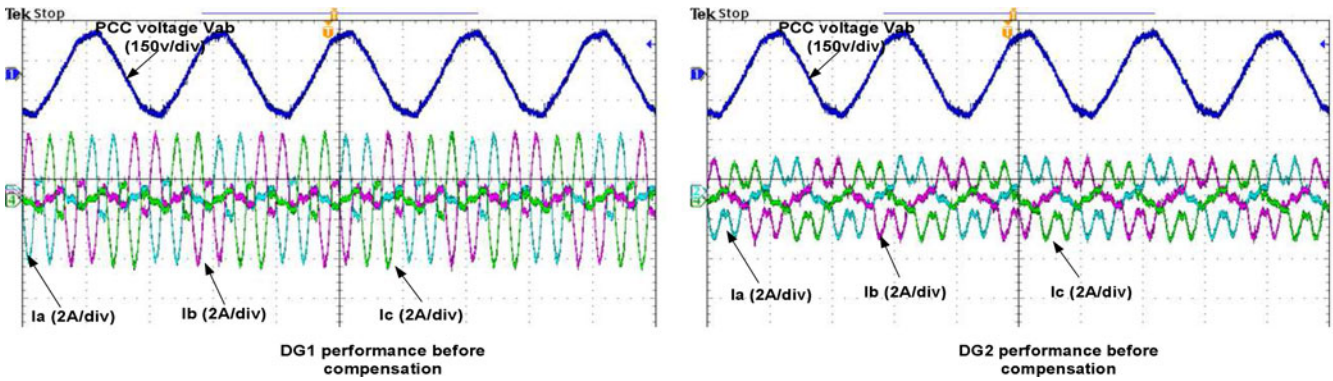

Fig. 15. Performance of the conventional droop control in a microgrid with harmonic load (load Type II).

current is at these two harmonic frequencies. However, the virtual impedance can also be controlled at higher harmonic frequencies if it is needed.

Case III (With generalized loads): To test the effectiveness of the proposed method in a microgrid with generalized PCC loads. An imbalanced *RL* load and a three-phase diode rectifier are connected to PCC at the same time. The load sharing performance using only conventional droop control method is presented in Fig. 17. It is obvious that DG1 shares more load current as its feeder impedance is smaller.

To reduce the microgrid power sharing errors, the compensation flags in the central controller are generated in the sequence of reactive power compensation, imbalance power compensation, and harmonic power compensation. After the adjustment of DG virtual impedance at the corresponding fundamental positive sequence, fundamental negative sequence, and harmonic frequencies, the current sharing performance is illustrated in

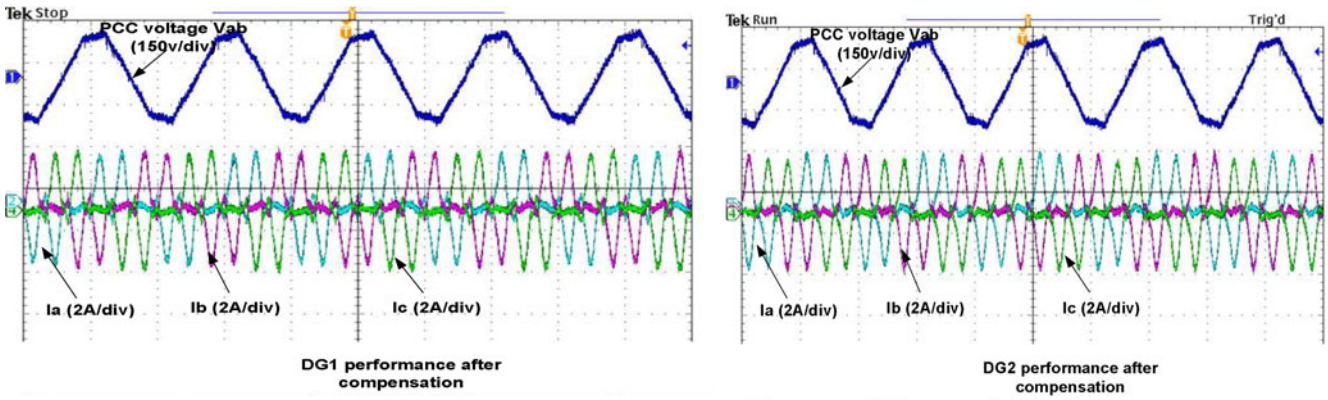

Fig. 16. Performance of the proposed compensation method in a microgrid with harmonic load (load Type II in Fig. 12).

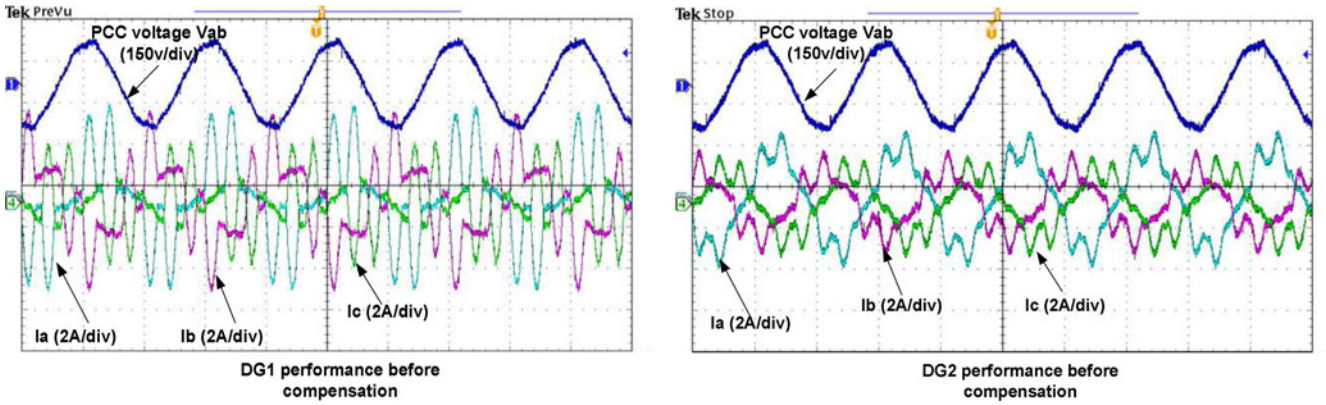

Fig. 17. Performance of the conventional droop control method in a microgrid with generalized load (load Type III in Fig. 12).

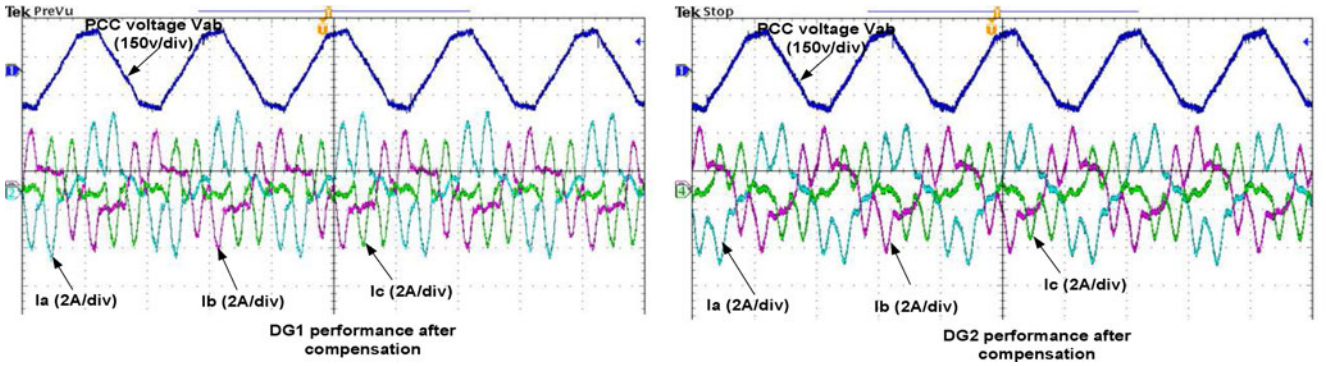

Fig. 18. Performance of the proposed compensation method in a microgrid with generalized load (load Type III in Fig. 12).

Fig. 18. Compared to the performance in Fig. 17, it can be seen that the proposed method is effective to address the power sharing errors in a microgrid with generalized loads.

VI. Conclusion

This paper discusses an enhanced power sharing scheme for islanding microgrids. The proposed method utilizes the frequency droop as the link to compensate reactive, imbalance, and harmonic power sharing errors. Specifically, the frequency droop control with additional disturbance is used to produce some real power sharing variations. These real power variations are used to adjust the DG unit virtual impedances at fundamental positive sequence, fundamental negative sequence, and harmonic frequencies. With the interactions between the transient frequency droop control and the variable DG virtual impedance, the impact of unknown feeder impedances can be properly compensated and an accurate power sharing is achieved at the steady state. Comprehensive simulated and experimental results from

a low-voltage microgrid prototype verified the effectiveness of the proposed scheme.

Note that the same virtual impedance is used at negative sequence fifth and positive sequence seventhharmonics, as typically they are dominate harmonic components in an islanding microgrid. To realize better compensation performance, independent harmonic power-sharing error compensation at each harmonic order and each sequence can be developed in a similar way.

REFERENCES

[1] F. Blaabjerg, Z. Chen, and S. B. Kjaer, "Power electronics as efficient interface in dispersed power generation systems," *IEEE Trans. Power Electron.*, vol. 19, no. 5, pp. 1184–1194, May 2004.

[2] F. Blaabjerg, R. Teodorescu, M. Liserre, and V. A. Timbus, "Overview of control and grid synchronization for distributed power generation systems," *IEEE Trans. Ind. Electron.*, vol. 53, no. 5, pp. 1398–1409, Oct. 2006.

[3] Y. W. Li and C. N. Kao, "An accurate power control strategy for power-electronics-interfaced distributed generation units operating in a low-voltage multibus microgrid," *IEEE Trans. Power Electron.*, vol. 24, no. 2, pp. 2977–2988, Dec. 2009.

[4] J. M. Guerrero, L. G. Vicuna, J. Matas, M. Castilla, and J. Miret, "Output impedance design of parallel-connected UPS inverters with wireless load sharing control," *IEEE Trans. Ind. Electron.*, vol. 52, no. 4, pp. 1126–1135, Aug. 2005.

[5] J. M. Guerrero, L. G. Vicuna, J. Matas, M. Castilla, and J. Miret, "A wireless controller to enhance dynamic performance of parallel inverters in distributed generation systems," *IEEE Trans. Power Electron.*, vol. 19, no. 4, pp. 1205–1213, Sep. 2004.

[6] J. M. Guerrero, J. C. Vasquez, J. Matas, L.G. de Vicuna, and M. Castilla, "Hierarchical control of droop-controlled AC and DC microgrids—A general approach toward standardization," *IEEE Trans. Ind. Electron.*, vol. 55, no. 1, pp. 158–172, Jan. 2011.

[7] Y. W. Li, D. M. Vilathgamuwa, and P. C. Loh, "Design, analysis and real time testing of a controller for multibus microgrid system," *IEEE Trans. Power Electron.*, vol. 19, no. 5, pp. 1195–1204, Sep. 2004.

[8] J. He and Y. W. Li, "An enhanced microgrid load demand sharing strategy," *IEEE Trans. Power Electron.*, vol. 19, no. 5, pp. 1184–1194, May 2004.

[9] A. Tuladhar, H. Jin, T. Unger, and K. Mauch, "Control of parallel inverters in distributed AC power system with consideration of line impedance effect," *IEEE Trans. Ind. Appl.*, vol. 36, no. 1, pp. 131–138, Jan./Feb. 2000.

[10] D. De and V. Ramanarayanan, "Decentralized parallel operation of inverters sharing unbalanced and nonlinear loads," *IEEE Trans. Power Electron.*, vol. 25, no. 12, pp. 3015–3025, Dec. 2010.

[11] P. Rodríguez, A. Luna, I. Candlea, R. Mujal, R. Teodorescu, and F. Blaabjerg, "Multiresonant frequency-locked loop for grid synchronization of power converters under distorted grid conditions," *IEEE Trans. Ind. Electron.*, vol. 58, no. 1, pp. 127–138, Jan. 2011.

[12] P.-T. Cheng, C.-A. Chen, T.-L. Lee, and S.-Y. Kuo, "A cooperative imbalance compensation method for distributed generation interface converters," *IEEE Trans. Ind. Appl.*, vol. 45, no. 2, pp. 805–815, Mar./Apr. 2009.

[13] Q. Zhang, "Robust droop controller for accurate proportional load sharing among inverters operated in parallel," *IEEE Trans. Ind. Electron.*, vol. 60, no. 4, pp. 1281–1290, Apr. 2013.

[14] V. Gungor, D. Sahin, T. Kocak, S. Ergut, C. Buccella, C. Cecati, and G. Hancke, "Smart grid technologies: Communications technologies and standards," *IEEE Trans. Ind. Informat.*, vol. 7, no. 4, pp. 529–539, Nov. 2011.

[15] Y. Wang and Y. W. Li, "Three-phase cascaded delayed signal cancellation PLL for fast selective harmonic detection," *IEEE Trans. Ind. Electron*, vol. 60, no. 4, pp. 1452–1463, Apr. 2013.

[16] J. He and Y. W. Li, "Analysis, design and implementation of virtual impedance for power electronics interfaced distributed generation," *IEEE Trans. Ind. Appl.*, vol. 47, no. 6, pp. 2525–2538, Nov./Dec. 2011.

[17] E. A. A. Coelho, P. C. Cortizo, and P. F. D. Garcia, "Small-signal stability for parallel-connected inverters in stand-alone AC supply systems," *IEEE Trans. Ind. Appl.*, vol. 38, no. 2, pp. 533–542, Mar./Apr. 2002.

[18] M. Savaghebi, A. Jalilian, J. C. Vasquez, J. M. Guerrero, "Autonomous voltage unbalance compensation in an islanded droop controlled microgrid," *IEEE Trans. Ind. Electron.*, vol. 60, no. 4, pp. 1390–1402, Apr. 2013.

[19] Q-C. Zhong, "Harmonic droop controller to reduce the voltage harmonics of inverters," *IEEE Trans. Ind. Electron.*, vol. 60, no. 3, pp. 936–945, Mar. 2013.

[20] J. Svensson, M. Bongiorno, and A. Sannino, "Practical implementation of delayed signal cancellation for phase-sequence separation," *IEEE Trans. Power Del.*, vol. 22, no. 1, pp. 18–26, Jan. 2007.

[21] J. C. Vasquez, R. A. Mastromauro, J. M. Guerrero, and M. Liserre, "Voltage support provided by a droop-controlled multifunctional inverter," *IEEE Trans. Ind. Electron.*, vol. 56, no. 11, pp. 4510–4519, Nov. 2009.

[22] J. He and Y. W. Li, "Generalized closed-loop control schemes with embedded virtual impedances for voltage source converters with LC or LCL filter," *IEEE Trans. Power Electron.*, vol. 27, no. 4, pp. 1850–1861, Apr. 2012.

[23] P. C. Loh and D. G. Holmes, "Analysis of multi-loop control strategies for LC/CL/LCL-filtered voltage-source and current source inverters," *IEEE Trans. Ind. Appl.*, vol. 41, no. 2, pp. 644–654, Mar./Apr. 2005.

[24] T. L. Vandoorn, B. Renders, L. Degroote, B. Meersman, and L. Vandevelde, "Controllable harmonic current sharing in islanded microgrids: DG units with programmable resistive behavior toward harmonics," *IEEE Trans. Power Del.*, vol. 27, no. 3, pp. 1405–1414, Jul. 2012.

[25] L. Corradini, P. Mattavelli, M. Corradin, and F. Polo, "Analysis of parallel operation of uninterruptible power supplies loaded through long wiring cables," *IEEE Trans. Power Electron.*, vol. 25, no. 4, pp. 1046–1054, Apr. 2010.

[26] J. A. Jardini, C. M. V. Tahan, M. R. Gouvea, S. U. Ahn, and F.M. Figueiredo, "Daily load profiles for residential, commercial and industrial low voltage consumers," *IEEE Trans. Power Del.*, vol. 15, no. 1, pp. 375–380, Jan. 2000.

[27] I. J. Balaguer, Q. Lei, S. Yang, U. Supatti, and F. Z. Peng, "Control for grid-connected and intentional islanding operations of distributed power generation," *IEEE Trans. Power Electron.*, vol. 58, no. 1, pp. 147–157, Jan. 2011.

[28] Y. W. Li, "Control and resonance damping of voltage source and current source converters with LC filters," *IEEE Trans. Ind. Electron.*, vol. 56, no. 5, pp. 1511–1521, May 2009.

[29] N. Pogaku, M. Prodanovic, and T.C. Green, "Modeling, analysis and testing of autonomous operation of an inverter-based microgrid," *IEEE Trans. Power Electron.*, vol. 22, no. 2, pp. 613–625, Mar. 2007.

[30] M. Savaghebi, J. M. Guerrero, A. Jalilian, and J. C. Vasquez, "Hierarchical control scheme for voltage unbalance compensation in an islanded microgrid," in *Proc. 37th Annu. IEEE Conf. Ind. Electron.*, 2011, pp. 3014–3046.

[31] M. Savaghebi, J. M. Guerrero, A. Jalilian, J. C. Vasquez, and Tzung-Lin Lee, "Hierarchical control scheme for voltage harmonics compensation in an islanded droop-controlled microgrid," in *Proc. IEEE 9th Int. Conf. Power Electron. Drives*, 2011, pp. 89–94.

[32] X. Wang, F. Blaabjerg, Z. Chen, and J. M. Guerrero, "A centralized control architecture for harmonic voltage suppression in islanded microgrids," in *Proc. IEEE 37th Annu. Conf. Ind. Electron. Soc., Melbourne, Australia*, 2012, pp. 3070–3075.

[33] Q. Shafiee, J. M. Guerrero, and J. C. Vasquez, "Distributed secondary control for islanded microgrids—A new approach," *IEEE Trans. Power Electron.*, vol. 29, no. 2, pp. 1018–1031, Feb. 2014.

[34] J. M. Guerrero, M. Chandorkar, T. Lee, and P. C. Loh, "Advanced control architectures for intelligent microgrids—Part I: Decentralized and hierarchical control," *IEEE Trans. Ind. Electron.*, vol. 60, no. 4, pp. 1254–1262, Apr. 2013.

[35] J. M. Guerrero, P. C. Loh, T. Lee, and M. Chandorkar, "Advanced control architectures for intelligent microgrids—Part II: Power quality, energy storage, and AC/DC microgrids," *IEEE Trans. Ind. Electron.*, vol. 60, no. 6, pp. 1263–1270, Apr. 2013.

[36] Tzung-lin Lee and Po-Tai Cheng, "Design of a new cooperative harmonic filtering strategy for distributed generation interface converters in an islanding network," *IEEE Trans. Power. Electron.*, vol. 22, no. 5, pp. 1919–1927, May 2007.

[37] C-.T. Lee, C-.C. Chu, and P-.T. Cheng, "A new droop control method for the autonomous operation of distributed energy resource interface

converters," *IEEE Trans. Power. Electron.*, vol. 28, no. 4, pp. 1980–1993, Apr. 2013.

[38] K. D. Brabandere, B. Bolsens, J. V. D. Keybus, A. Woyte, J. Driesen, and R. Belmans, "A voltage and frequency droop control method for parallel inverters," *IEEE Trans. Power. Electron.*, vol. 22, no. 4, pp. 1107–1115, Jul. 2007.

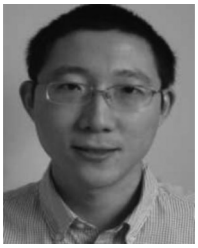

Jinwei He received the B.Eng. degree from Southeast University, Nanjing, China, in 2005, the M.Sc. degree from the Institute of Electrical Engineering, Chinese Academy of Sciences, China, in 2008, and the Ph.D. degree from the University of Alberta, Edmonton, Canada, in 2013, all in electrical engineering.

From 2008 to 2009, he was a Power Electronics Engineer with China Electronics Technology Group Corporation. In 2012, he worked as a Visiting Scholar at the Institute of Energy Technology, Aalborg University. He has been working as a Power Electronics Engineer at Accuenergy Canada Inc., Toronto, ON, Canada, since 2013. His research interests include variable frequency drive of railway traction motors, linear electric machine design, power quality, active filters, and high power electronics applications in distributed power generation and ground transportation.

Yun Wei Li (S'04–M'05–SM'11) received the B.Sc. degree in engineering degree in electrical engineering from Tianjin University, Tianjin, China, in 2002, and the Ph.D. degree from Nanyang Technological University, Singapore, in 2006.

In 2005, he was a Visiting Scholar with Aalborg University, Denmark. From 2006 to 2007, he was a Postdoctoral Research Fellow at Ryerson University, Canada. In 2007, he worked at Rockwell Automation Canada and later joined the Department of Electrical and Computer Engineering, University of Alberta, Edmonton, Canada in the same year. He is currently an Associate Professor at the University of Alberta. His research interests include distributed generation, microgrid, renewable energy, high power converters, and electric motor drives.

Dr. Li serves as an Associate Editor for the IEEE TRANSACTIONS ON POWER ELECTRONICS and the IEEE TRANSACTIONS ON INDUSTRIAL ELECTRONICS. He also worked as a Guest Editor for the IEEE TRANSACTIONS ON INDUSTRIAL ELECTRONICS special session on distributed generation and microgrids. He received the 2013 Richard M. Bass Outstanding Young Power Electronics Engineer Award from IEEE Power Electronics Society.

Frede Blaabjerg (S'86–M'88–SM'97–F'03) received the Ph.D. degree from Aalborg University, Aalborg, Denmark, in 1992.

He was with ABB-Scandia, Randers, Denmark, from 1987 to 1988. He became an Assistant Professor in 1992, an Associate Professor in 1996, and a Full Professor of power electronics and drives in 1998. His current research interests include power electronics and its applications such as in wind turbines, PV systems, reliability, harmonics, and adjustable speed drives.

Dr. Blaabjerg received 15 IEEE Prize Paper Awards, the IEEE Power Electronics Society Distinguished Service Award in 2009, the EPE-PEMC Council Award in 2010, the IEEE William E. Newell Power Electronics Award 2014, and the Villum Kann Rasmussen Research Award 2014. He was an Editor-in-Chief of the IEEE TRANSACTIONS ON POWER ELECTRONICS from 2006 to 2012. He has been a Distinguished Lecturer for the IEEE Power Electronics Society from 2005 to 2007 and for the IEEE Industry Applications Society from 2010 to 2011.